

## Supporting Information

# Multifunctional nanocomposites mediated novel hydrogel for diabetic wound repair

*Yingjuan Zhou<sup>al</sup>, Jiaxin Yang<sup>bl</sup>, Yan Li<sup>cl</sup>, Xin Shu<sup>d</sup>, Yucen Cai<sup>a</sup>, Ping Xu<sup>a</sup>, Wenyan Huang<sup>a</sup>,  
Zhangyou Yang<sup>a\*</sup> and Rong Li<sup>b\*</sup>*

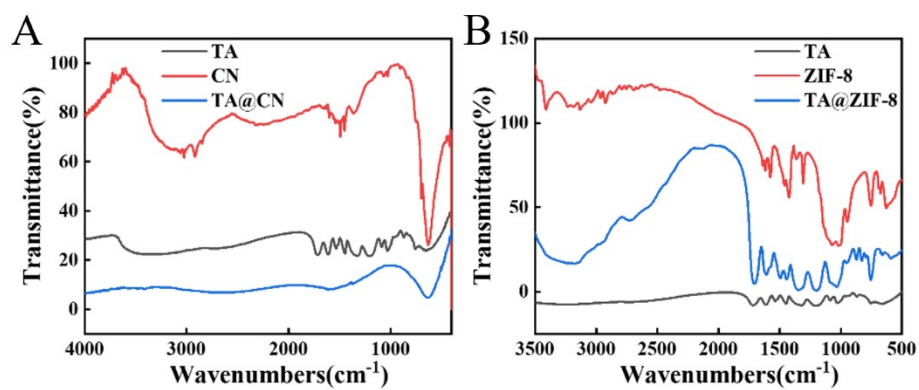
<sup>a</sup>Center for Pharmaceutical Formulation and Nanomedicine Research,  
College of Pharmacy, Chongqing Medical University, Chongqing 400016, P.R. China  
E-mail: yangzhangyou@cqmu.edu.cn (Zhangyou Yang)

<sup>b</sup>Institute of Combined Injury, State Key Laboratory of Trauma, Burns and Combined Injury,  
Military Key Laboratory of Nanomedicine, Department of Military Preventive Medicine,  
Army Medical University, Chongqing, 400038, People's Republic of China;  
E-mail: [lrong361@126.com](mailto:lrong361@126.com) (Rong Li)

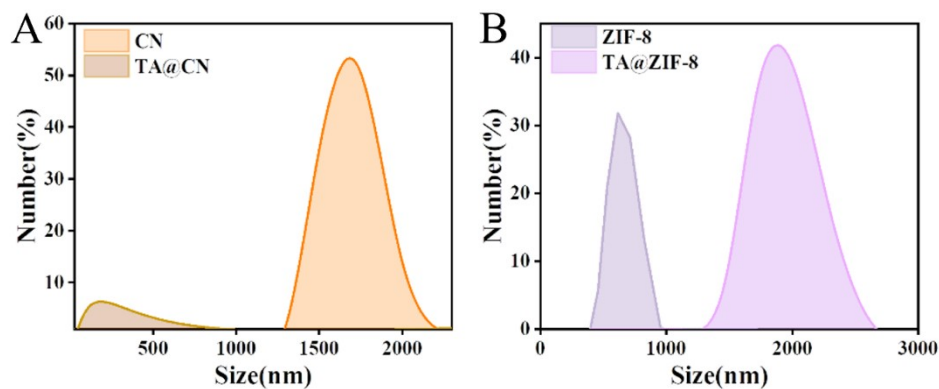
<sup>c</sup>Chongqing Engineering Research Center of Pharmaceutical Sciences, Chongqing Medical  
and Pharmaceutical College, Chongqing, 401331 PR China.

<sup>d</sup>College of pharmacy, Chongqing Medical and Pharmaceutical College

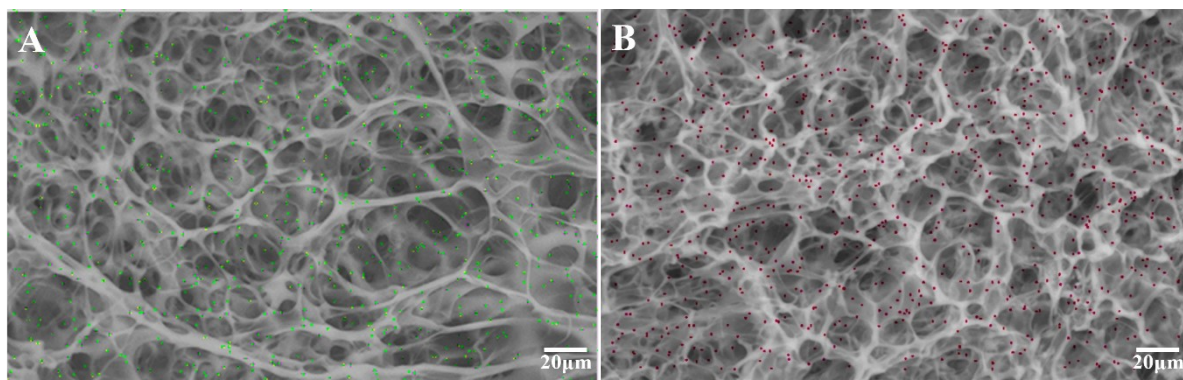
<sup>†</sup>These authors contributed equally to this work



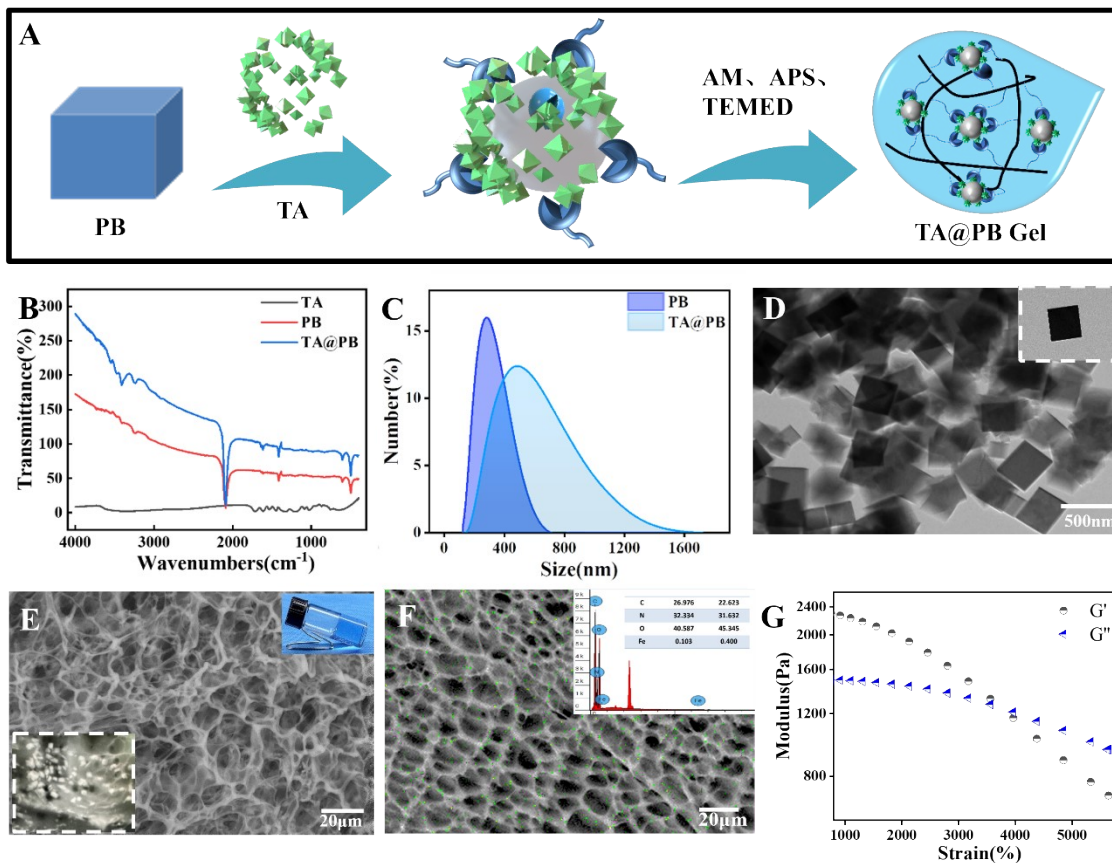
**Fig. S1.** Fourier infrared spectroscopy of different nanoparticles and tannic acid (TA). (A) CNPs; (B) ZIF-8.



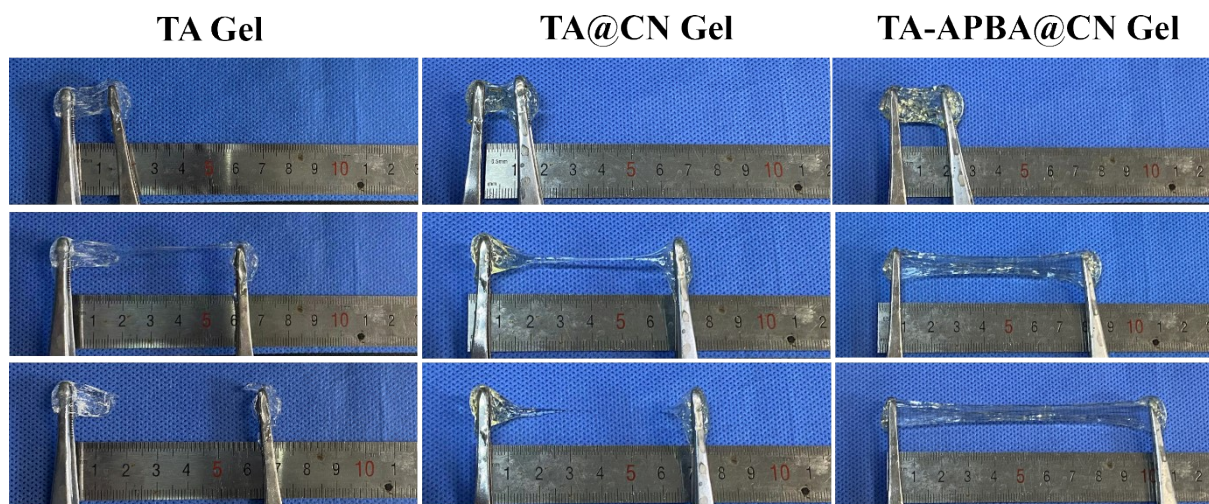
**Fig. S2.** DLS characterization of different nanoparticles before and after tannic acid (TA) modification. (A) CNPs; (B) ZIF-8.



**Fig. S3.** (A) SEM elemental scanning of TA@CN Gel; (B) TA@ZMG Gel.



**Fig. S4.** Schematic of Prussian blue nanoparticle-mediated hydrogel synthesis and its characterization



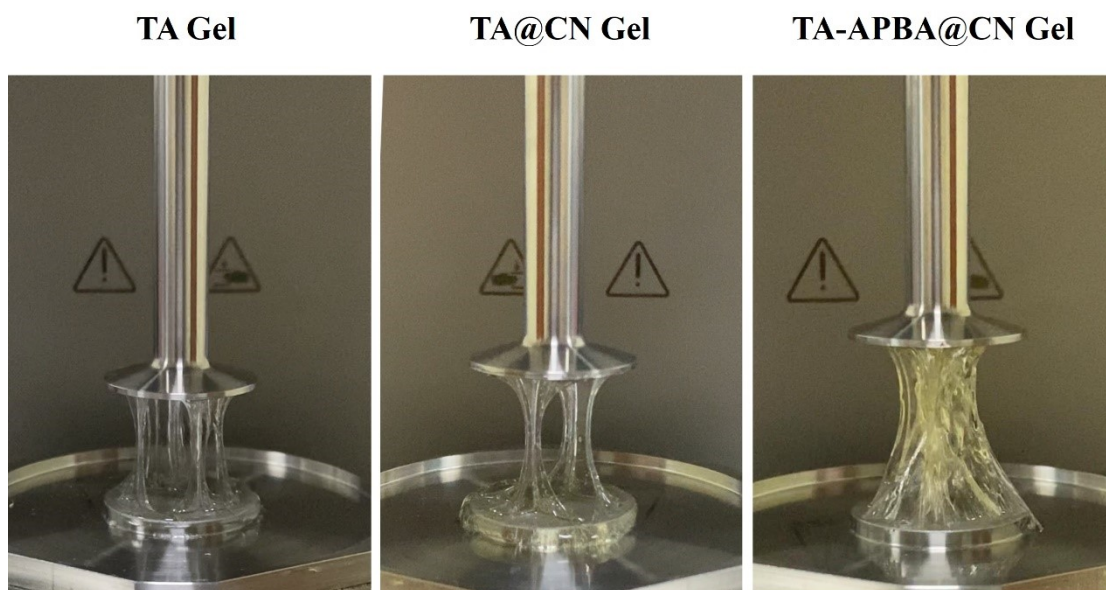


**Fig. S5.** Effect of nanoparticles and borate ester bonds on the mechanical properties of hydrogels.

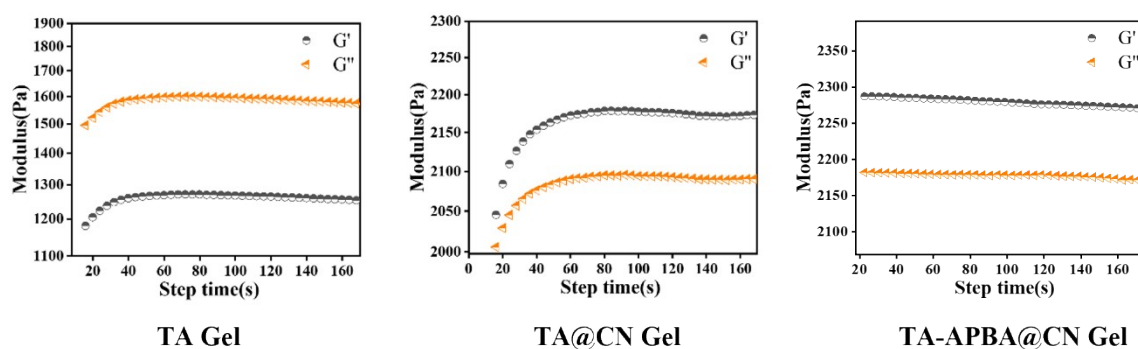


**Fig. S6.** Effect of nanoparticles and borate ester bond on rheological properties of hydrogels.

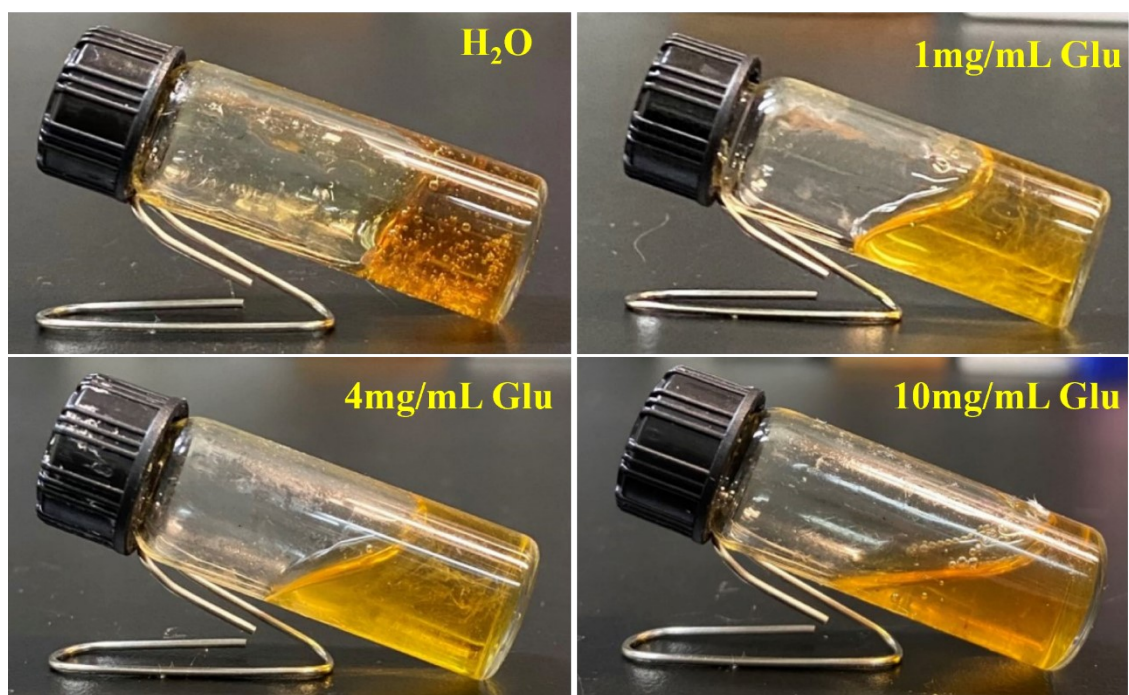
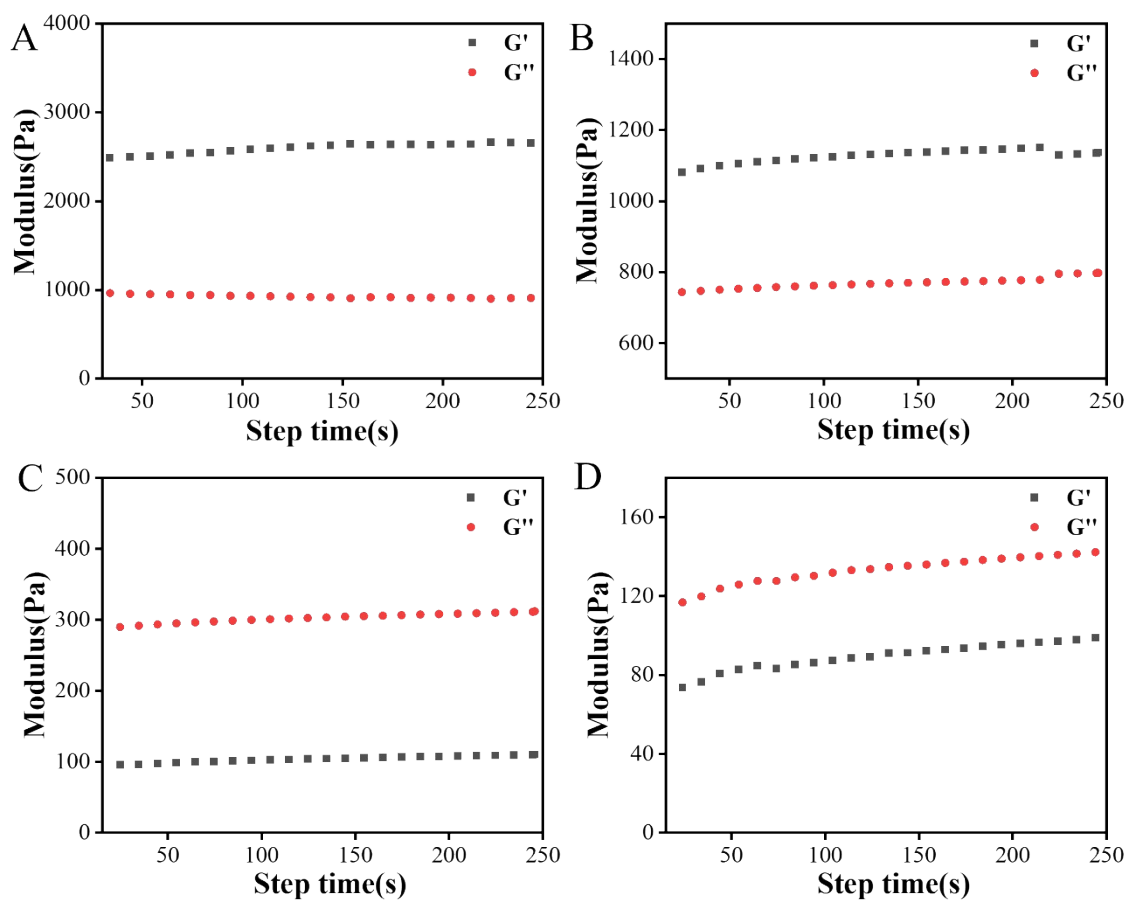
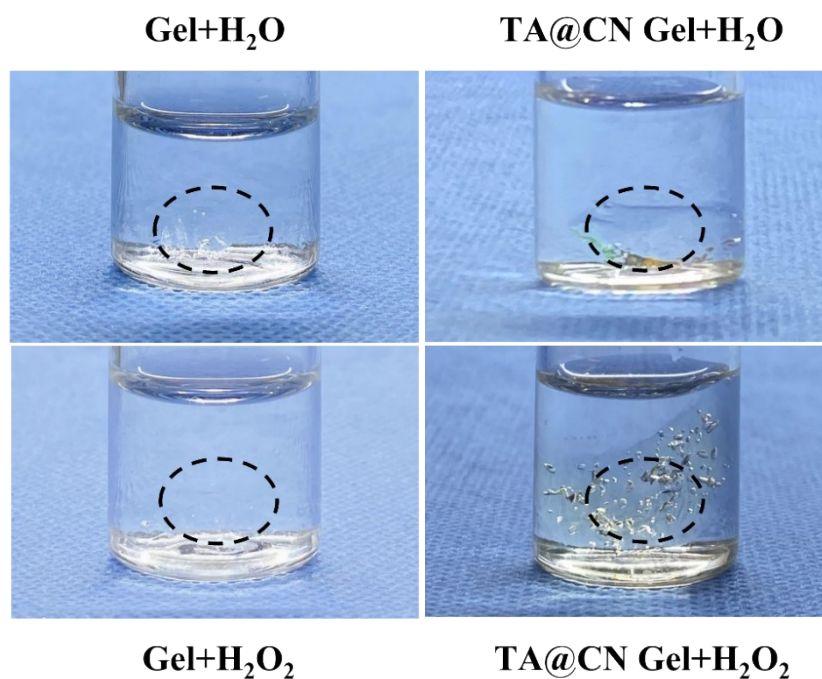


Fig. S7. Degradation of hydrogels in different concentrations of glucose.



**Fig. S8.** Storage moduli( $G'$ ) and loss moduli( $G''$ ) of hydrogel after degradation in different concentrations of glucose solutions.(A) $H_2O$ ;(B)  $1\text{ mg mL}^{-1}$  glucose solution;(C)  $4\text{ mg mL}^{-1}$  glucose solution;(D)  $10\text{ mg mL}^{-1}$  glucose solution.



**Fig. S9.** Pictures of oxygen production by adding  $H_2O$  and  $H_2O_2$  to different materials.

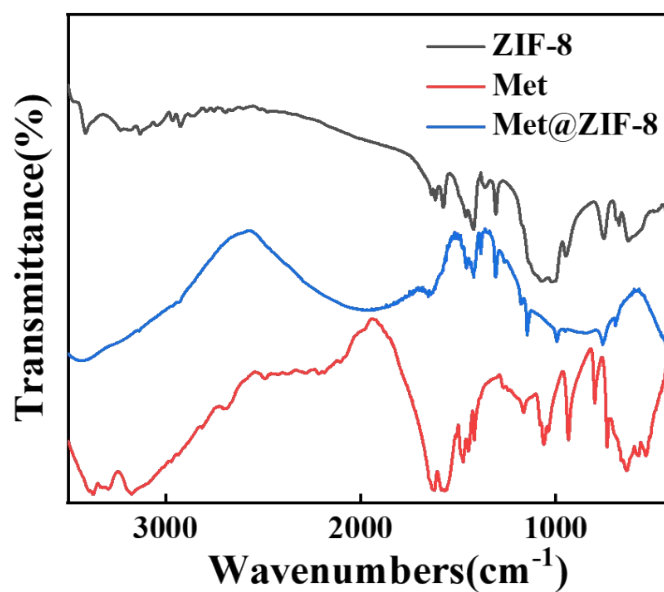


**Fig. S10.** The FIRT results showed a characteristic absorption peak of guanidine group at 1168 nm confirming the successful loading of metformin.

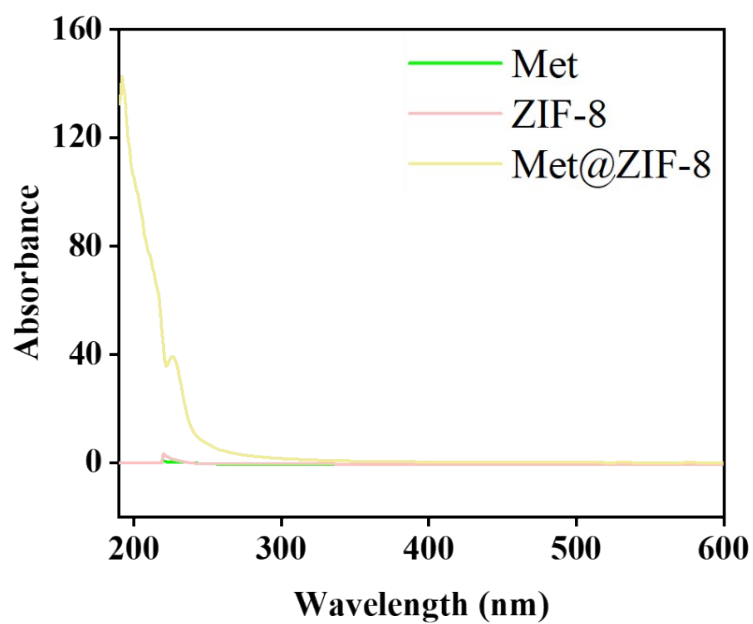


**Fig. S11.**Uv absorption of ZIF-8 nanoparticles, metformin and ZIF-8 loaded with metformin. The absorption peak showed that metformin was successfully loaded.

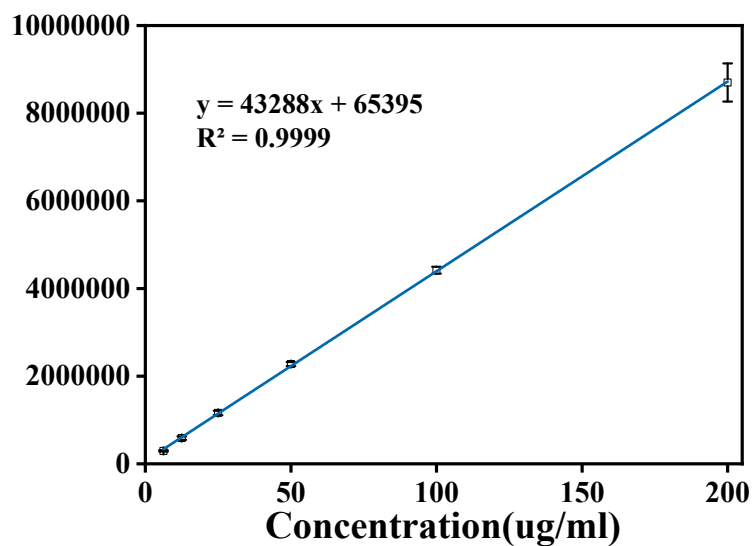


**Fig. S12.** Standard curve of metformin hydrochloride by HPLC.

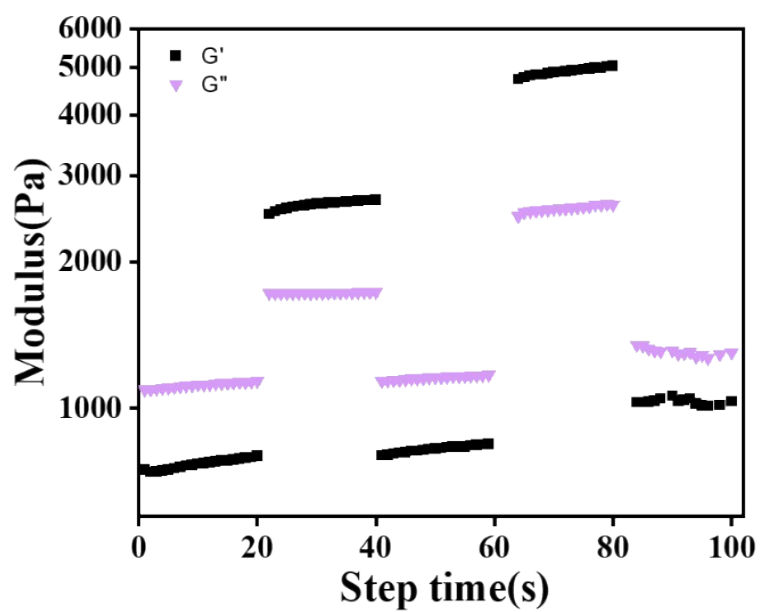


Fig. S13. Self-healing properties of TA@ZMG Gel.

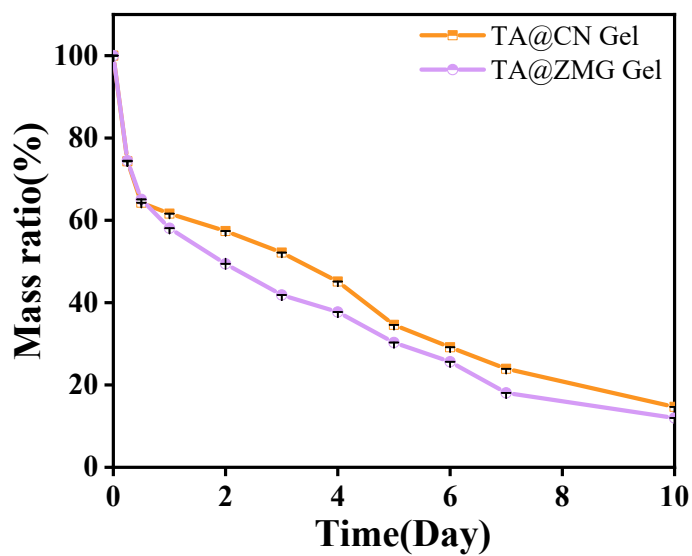
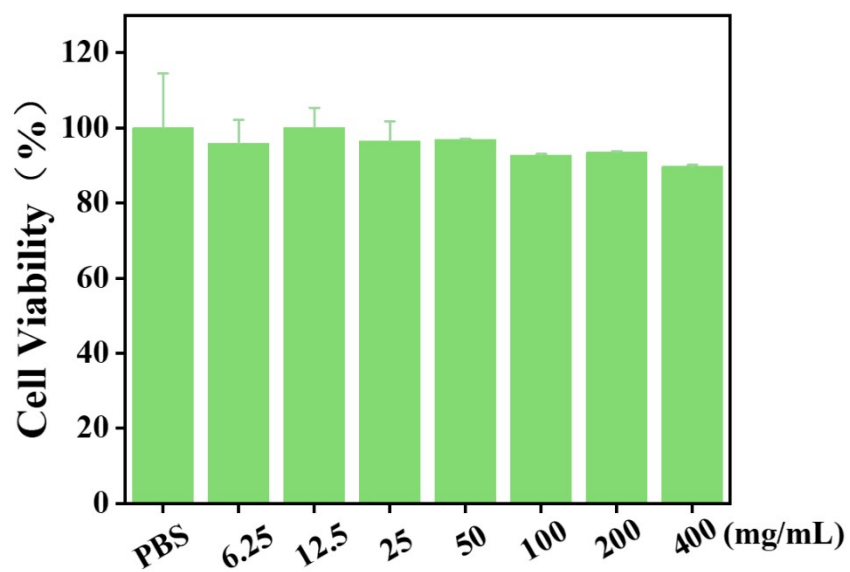
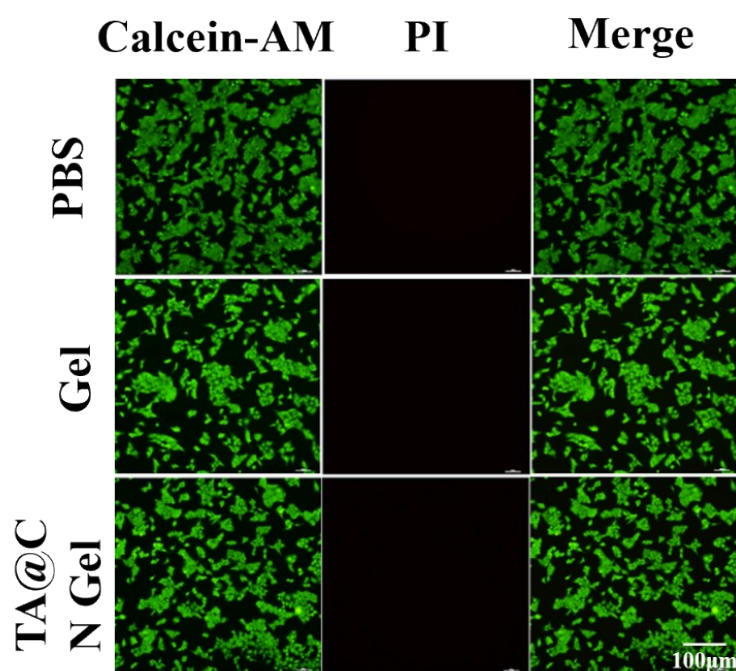


Fig. S14. Degradation of TA@CN Gel and TA@ZMG Gel.

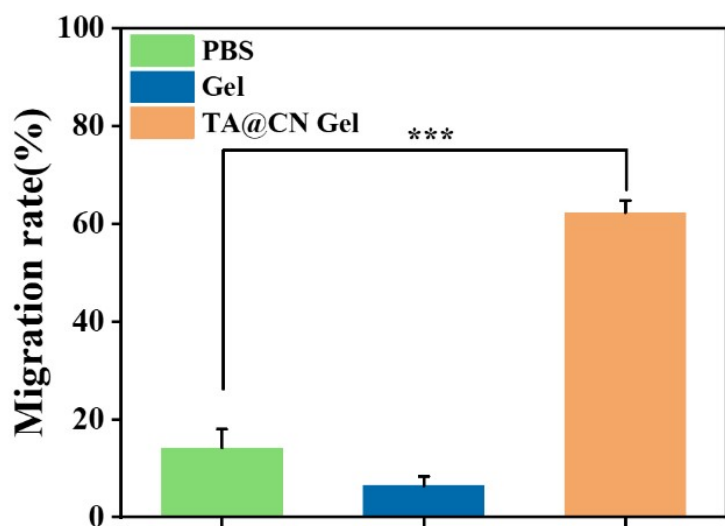
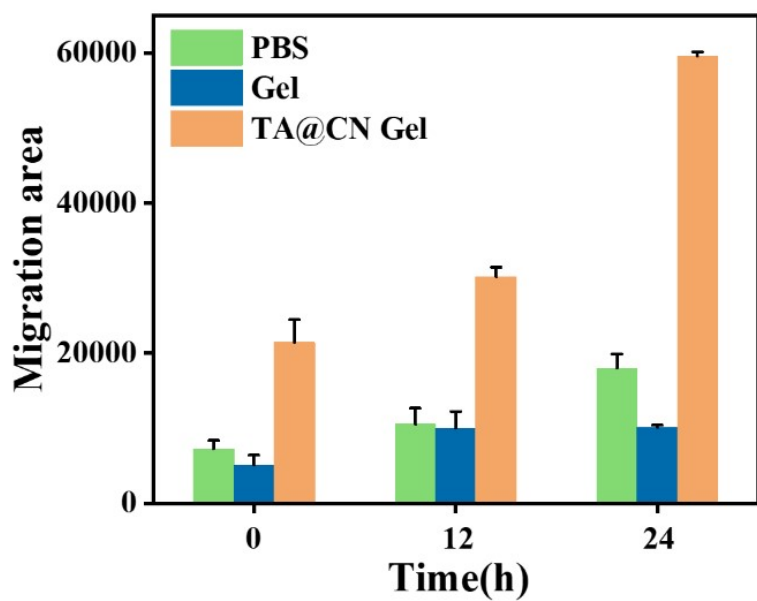




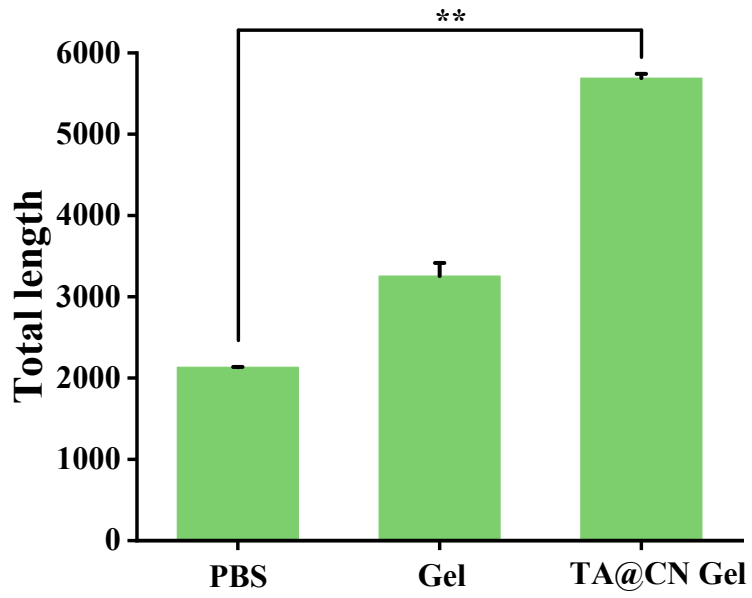
**Fig. S15.** Cell viability after 24 h treatment with different concentrations of TA@CN Gel.



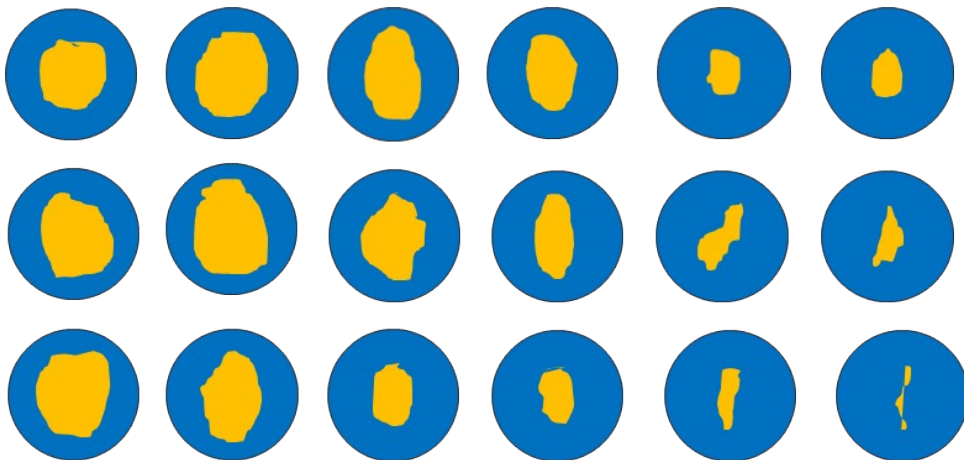
**Fig. S16.** Calcein -AM/PI cell staining in different treatment groups.



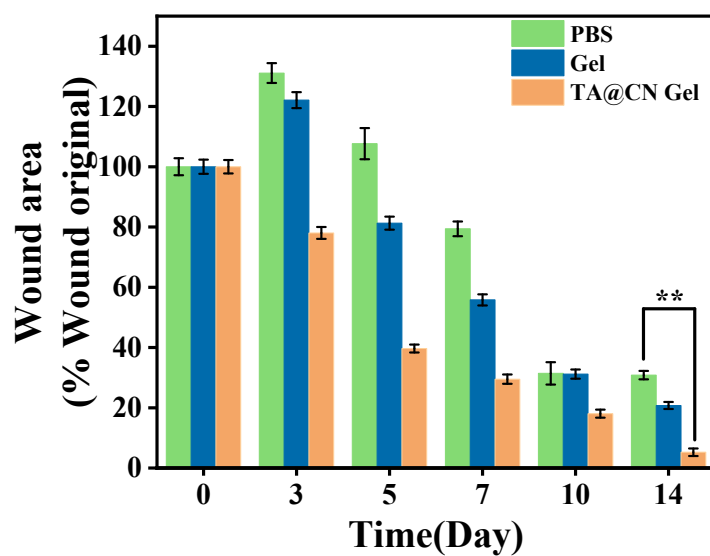
**Fig. S17.** Quantification of cell migration area and cell migration rate of different treatment groups.



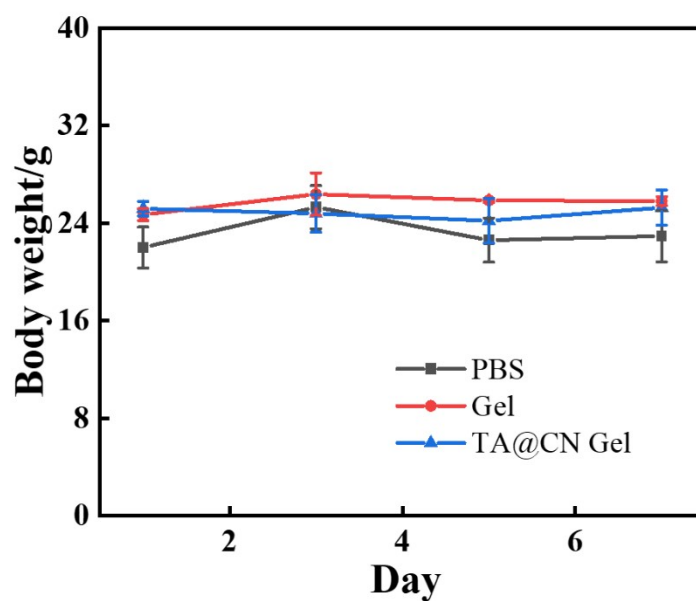
**Fig. S18.** Quantification of vessel length.



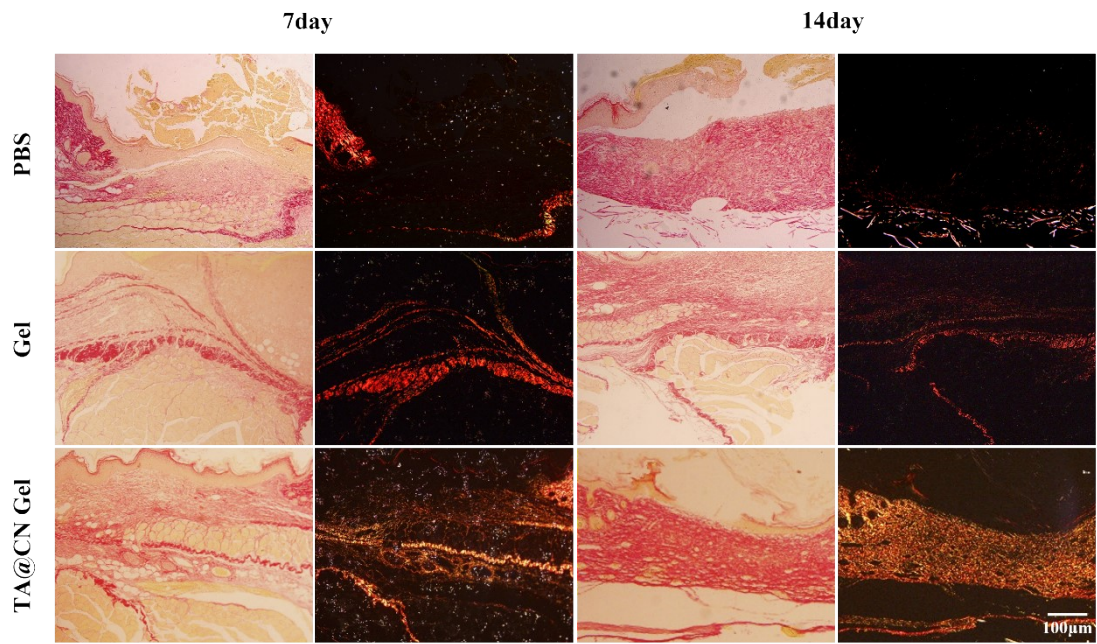
**Fig. S19.** Image J simulation analysis of wound size.



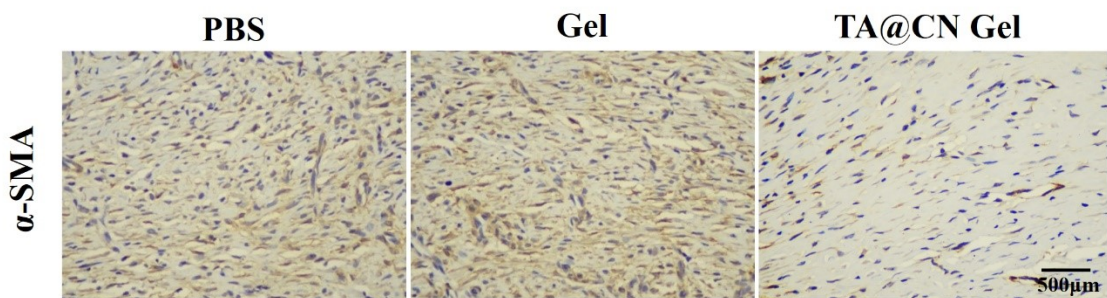
**Fig. S20.** Quantification of wound area at 3, 5, 7, 10 and 14 days for different treatments.



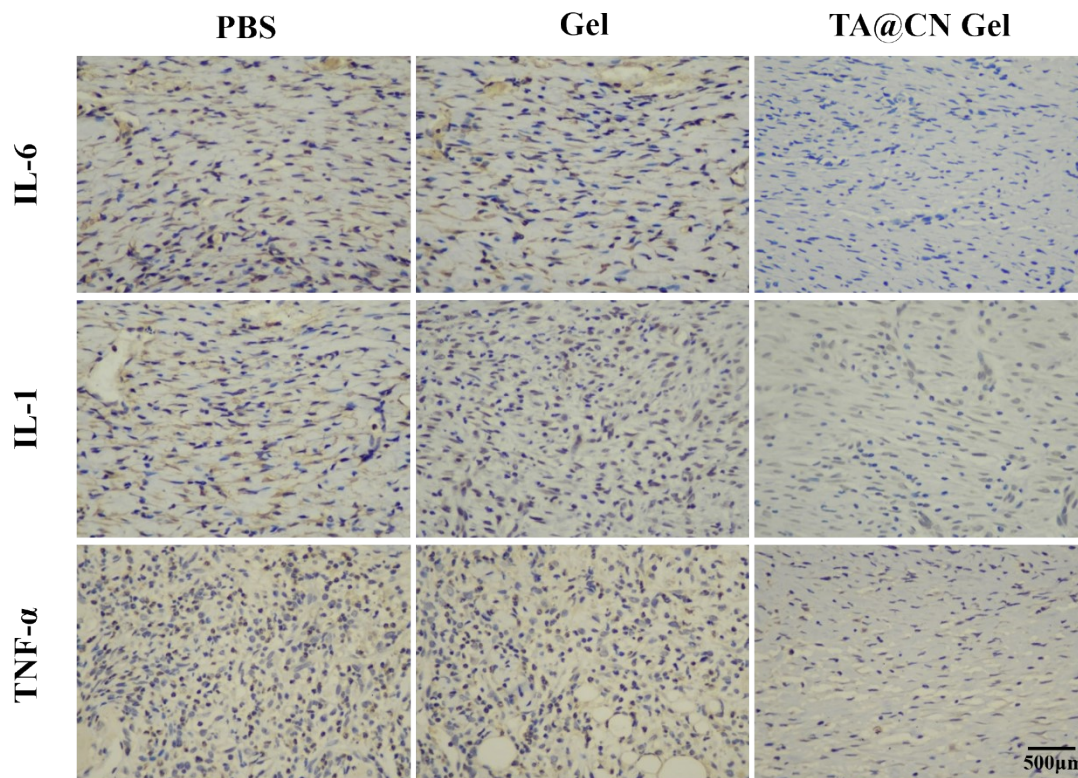
**Fig. S21.** Weight changes of mice in different groups during treatment.



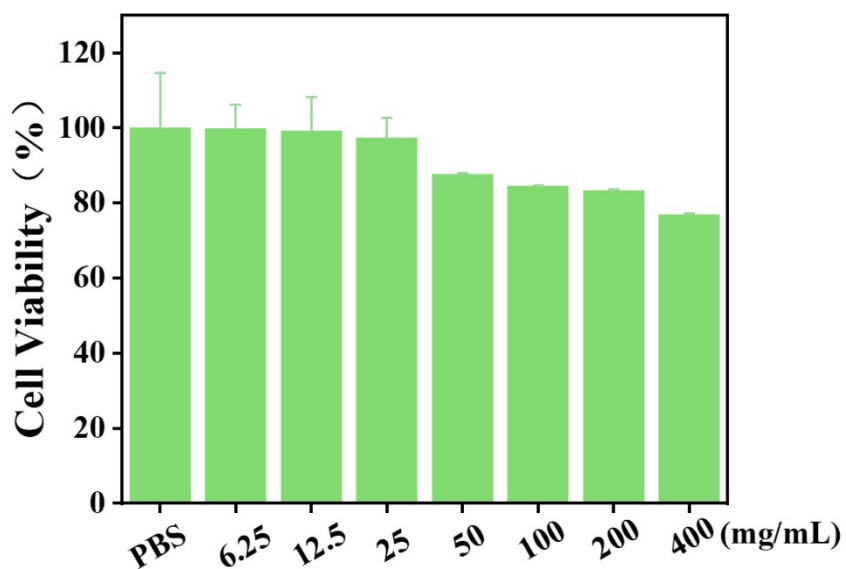
**Fig. S22.** Polarized optical microscope images of birefringent collagen at 7,14 days.



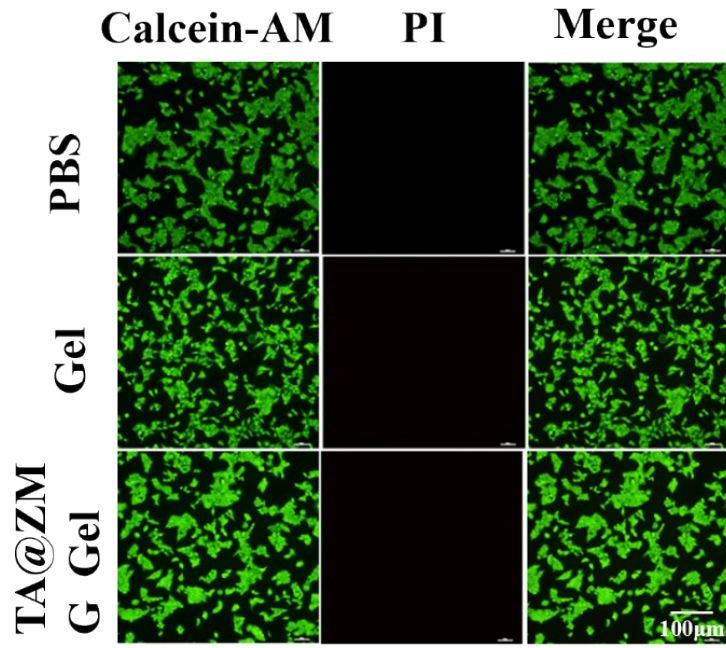
**Fig. S23.**  $\alpha$ -SMA histochemical staining of the wound on day 14.



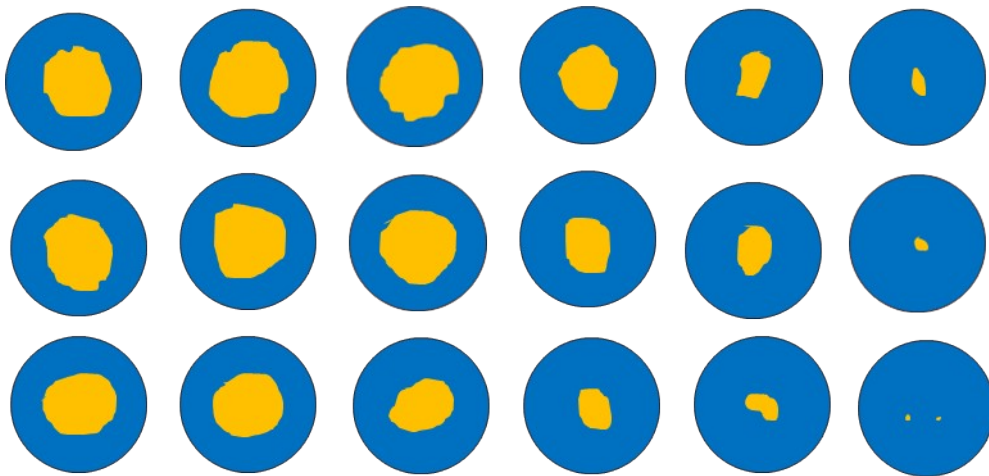
**Fig. S24.** Immunohistochemical staining of IL-6 $\beta$ , IL-1 and TNF- $\alpha$  expressed in wounds at 14 day.



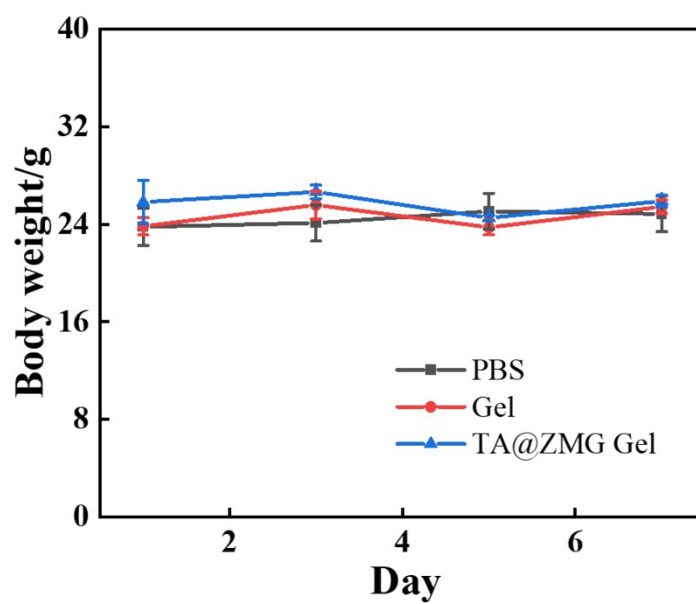
**Fig. S25.** Cell viability after 24 h treatment with different concentrations of TA@ZMG Gel.



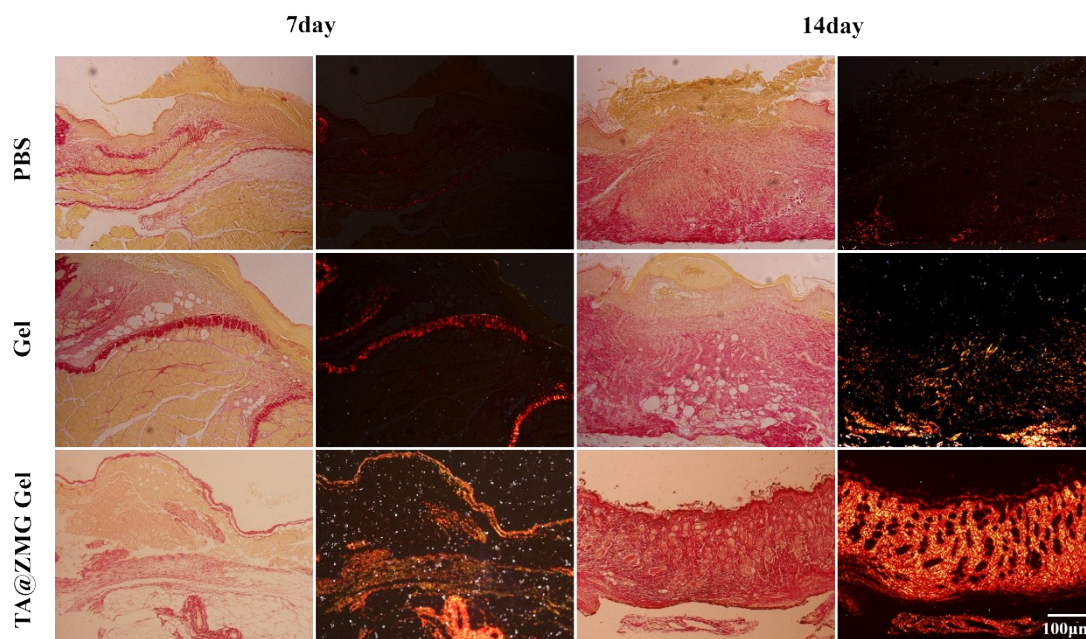
**Fig. S26.** Calcein -AM/PI cell staining in different treatment groups.



**Fig. S27.** Image J simulation analysis of wound size.

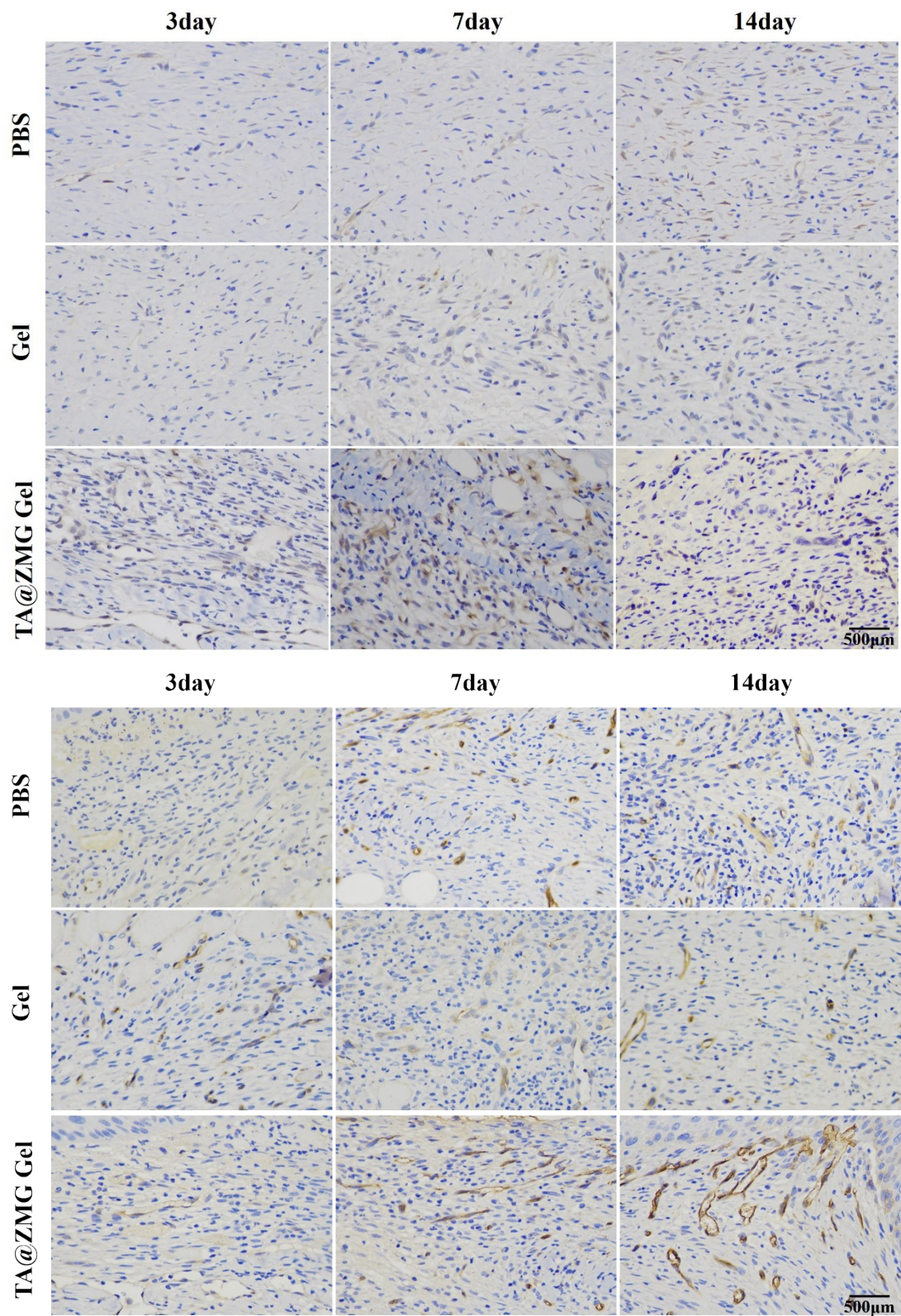


**Fig. S28.** Changes of body weight in PBS, Gel and TA@ZMG Gel groups during treatment.

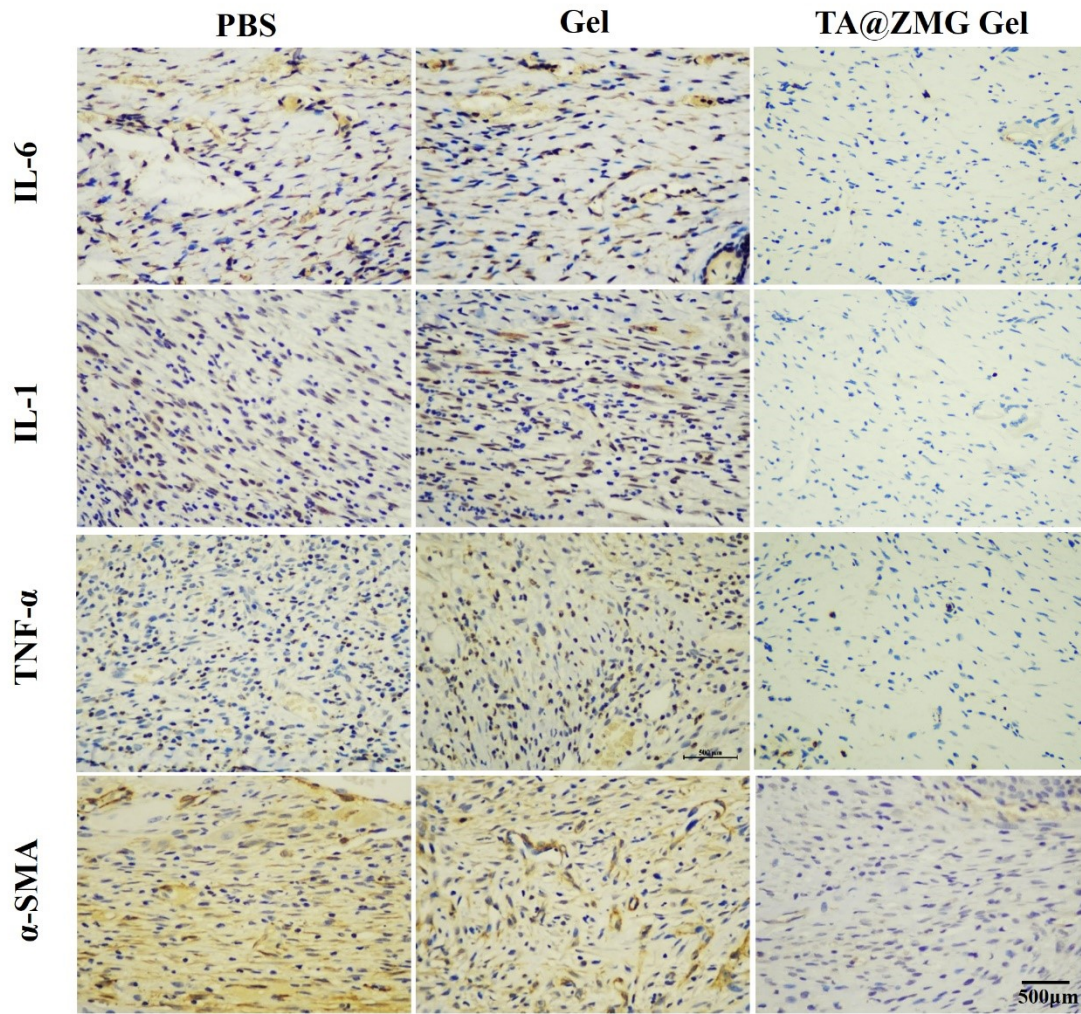


**Fig. S29.** Diabetic wound tissues were stained with bitter red collagen on different days (7,14 days).

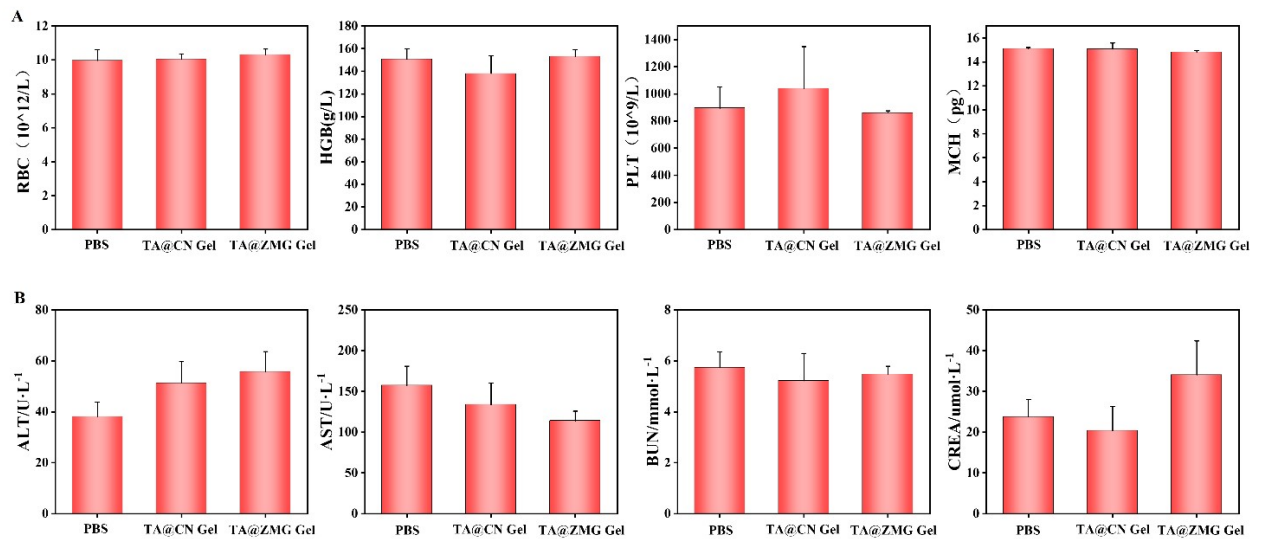




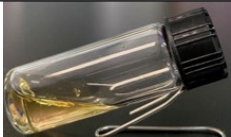


**Fig. S30.** VEGF and CD31 histochemical staining.



**Fig. S31.** Immunohistochemical staining of IL-6 $\beta$ , IL-1,  $\alpha$ -SMA and TNF- $\alpha$  expressed in wounds at 14 day.



**Fig. S32.** *In vivo* safety assessment. (A) Results of routine blood analysis: red blood cells (RBC), hemoglobin (HGB), platelets (PLT) and mean corpuscular hemoglobin (MCH). (B) Serum levels of typical lipid markers. ALT, alanine aminotransferase; AST, aspartate aminotransferase; BUN, blood urea nitrogen; CRE, blood creatinine.

AM	2M	5M	7M
TA : APBA	1 : 10	1 : 10	1 : 10
APS:TEMED	10 : 1	10 : 1	10 : 1
Hydrogel Properties			

**Table S1.** Experiments on the conditions of hydrogel formation in different ratios.